

Simulation of the Quantum Heat Engine in the Quantum Register

Marcin Ostrowski^[0000-0001-8985-8123]

*Lodz University of Technology
Institute of Information Technology
Wólczańska 215, 90-924 Łódź, Poland
marcin.ostrowski@p.lodz.pl*

DOI:10.34658/9788366741928.59

Abstract. *This paper investigates whether a quantum computer can efficiently simulate the transfer of excitation between a pair of quantum systems with energy loss caused by photon or phonon emission. The main contribution of our work is an algorithm that enables the simulation of time evolution of such a system, implemented on a standard two-input gates. The paper examines the properties of the proposed algorithm and then compares the obtained results with theoretical predictions.*

Keywords: *quantum simulations, excitation transfer, quantum heat engine*

1. Introduction

In the near future, quantum calculations are likely to make a major contribution to the development of informatics [1]. Nowadays, some institutions claim to have a quantum computer and offer its computing power. Therefore, it is worth examining the properties of such a machine.

For many years, we have known Shor [2] and Grover [3] algorithms which are faster than their best classical counterparts. Another promising application of a quantum computer is quantum simulation [4], i.e. the computer modeling of behavior of physical quantum systems. It gives the possibility of effective modeling quantum processes, which is not possible using classical computers. Quantum computers can simulate a wide variety of quantum systems, including fermionic lattice models [5], quantum chemistry and quantum field theories [6].

In the present study, we consider a quantum system (the system A from Fig. 1), which returns to the ground state with partial energy transfer to another system (the system B). The rest of the energy is emitted as a photon or phonon (the system C). The process described above is equivalent to operation of the quantum heat engine. It occurs during optical pumping of the laser or during photosynthesis [7], where the energy of an absorbed photon is transferred at a loss in many steps between successive carriers.

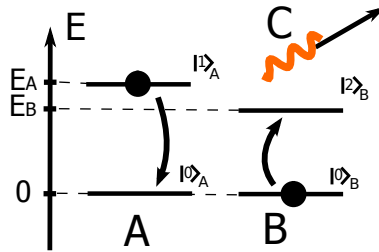


Figure 1. Energy transfer between subsystems A (hot reservoir) and B (quantum heat engine) with emission of photon C (cold reservoir). Source: own work.

The main purpose of our work is to investigate whether this phenomenon could be simulated in the quantum register. In the future, the ability to simulate such phenomena in a quantum computer may prove useful in the process of designing new quantum heat engines. Due to its low complexity level, the algorithm presented here may be used as a part of a more complex simulation.

The results presented here are preliminary. The issue we are considering is related to the optimization of the energy transport process in biological and artificial systems. It is claimed that the process of photosynthesis gains light-harvesting efficiency by exploiting the phenomenon of quantum coherence [8]. This involves the superpositions of electronic quantum states, which seem able to explore many energy-transmitting pathways at once.

2. Description of the simulated system

Let us consider a complex quantum system that is composed of three parts: A, B and C. The subsystem B (quantum heat engine) has three nondegenerate energy levels, which are denoted as follows: $|0\rangle_B$, $|1\rangle_B$ and $|2\rangle_B$. Energies of these states are equal to $E_0 = 0$, $E_1 > 0$ and $E_2 = E_B > 0$, respectively. Subsystems A (hot reservoir) and C (cold reservoir) have two nondegenerate energy levels. Stationary states of the system A we denote by $|0\rangle_A$ and $|1\rangle_A$. We assign them energies equal to $E_0 = 0$ and $E_A > 0$, respectively. Analogously, stationary states of the system C we denote by $|0\rangle_C$, $|1\rangle_C$, and we assign them energies equal to $E_0 = 0$ and $E_C > 0$, respectively. Full structure of the system is shown in Fig. 2.

The free Hamiltonian of the system we can write in the following form:

$$\hat{H}_0 = E_A \hat{a}^\dagger \hat{a} + E_1 \hat{b}_1^\dagger \hat{b}_1 + E_2 \hat{b}_2^\dagger \hat{b}_2 + E_C \hat{c}^\dagger \hat{c}, \quad (1)$$

where increasing and decreasing energy operators are defined as follows:

$$\hat{a}^\dagger |0\rangle_A = |1\rangle_A, \quad \hat{b}_1^\dagger |0\rangle_B = |1\rangle_B, \quad \hat{b}_2^\dagger |2\rangle_B = |1\rangle_B, \quad \hat{c}^\dagger |0\rangle_C = |1\rangle_C, \quad (2)$$

$$\hat{a}|1\rangle_A = |0\rangle_A, \quad \hat{b}_1|1\rangle_B = |0\rangle_B, \quad \hat{b}_2|1\rangle_B = |2\rangle_B, \quad \hat{c}|1\rangle_C = |0\rangle_C.$$

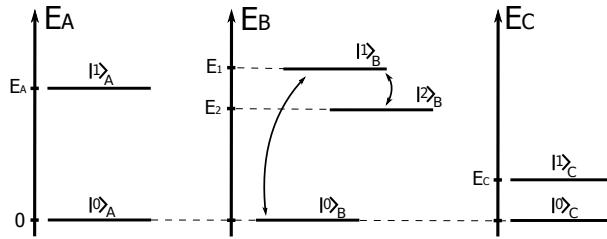


Figure 2. Scheme of the simulated systems. Source: own work.

The Hamiltonian of interaction we choose in the following form:

$$\hat{H}_{int} = g_1 \hat{a}^\dagger \hat{b}_1 + g_1^* \hat{a} \hat{b}_1^\dagger + g_2 \hat{c}^\dagger \hat{b}_2 + g_2^* \hat{c} \hat{b}_2^\dagger, \quad (3)$$

where g_1 and g_2 are coupling constants.

For the Hamiltonian (3) interaction between subsystems A and B generate the transition $|1\rangle_A|0\rangle_B \leftrightarrow |0\rangle_A|1\rangle_B$. Analogously, interaction between subsystems B and C generate the transition $|1\rangle_B|0\rangle_C \leftrightarrow |2\rangle_B|1\rangle_C$.

In the presented system resonance occurs when:

$$E_A = E_2 + E_C. \quad (4)$$

If we additionally assume that

$$E_A = E_1, \quad (5)$$

resonances occur in AB and BC subsystems.

In this work we are also considering modification of the system presented above. We replace the $|1\rangle_C$ state with a band consisting $n_L - 1$ excited levels with energies given by:

$$E_{C_i} = \Delta E \cdot i \quad \text{for } i = 0, \dots, n_L - 1, \quad (6)$$

where $\Delta E = 2E_C/n_L$ is the distance between adjacent levels. Now the E_C is the middle energy level of the band. For this modification the Hamiltonian of interaction takes the form:

$$\hat{H}'_{int} = g_1 \hat{a}^\dagger \hat{b}_1 + g_1^* \hat{a} \hat{b}_1^\dagger + \sum_{i=1}^{n_L-1} (g_2 \hat{c}_i^\dagger \hat{b}_2 + g_2^* \hat{c}_i \hat{b}_2^\dagger), \quad (7)$$

where $\hat{c}_i^\dagger|0\rangle_C = |i\rangle_C$ and $\hat{c}_i|i\rangle_C = |0\rangle_C$. The extended system C simulate quantum field, which receives energy from the system B irreversibly.

3. Algorithm simulating time evolution of the system

In order to solve the Schrödinger equation for the Hamiltonian $\hat{H} = \hat{H}_0 + \hat{H}_{int}$ we use the time evolution operator in the form:

$$\hat{U}(dt) = \exp(-i\hat{H}dt/\hbar), \tag{8}$$

where dt is time step. For $dt \rightarrow 0$ operator given by Eq. (8) can be approximated as follows:

$$\begin{aligned} \hat{U}(dt) = & \exp(-iE_A\hat{a}^\dagger\hat{a}dt/\hbar)\exp(-i(E_1\hat{b}_1^\dagger\hat{b}_1 + E_2\hat{b}_2^\dagger\hat{b}_2)dt/\hbar)\exp(-iE_C\hat{c}^\dagger\hat{c}dt/\hbar) \\ & \times \exp(-i(g_1\hat{a}^\dagger\hat{b}_1 + g_1^*\hat{a}\hat{b}_1^\dagger)dt/\hbar)\exp(-i(g_2\hat{c}^\dagger\hat{b}_2 + g_2^*\hat{c}\hat{b}_2^\dagger)dt/\hbar). \end{aligned} \tag{9}$$

The above equation is equivalent to using the first-order Lie-Trotter formula with Trotter error $O(t^2)$. The simulation for a large time t is obtained by dividing the evolution into n Trotter steps ($t = n \cdot dt$).

The basic version of the algorithm (simulating the system from Fig. 2) is implemented in a four-qubit register, as shown in Fig 3. Stationary states of the subsystem B are encoded in B_1 and B_2 qubits in the following way: $|0\rangle_B \rightarrow |0\rangle_{B_2}|1\rangle_{B_1}$, $|1\rangle_B \rightarrow |1\rangle_{B_2}|1\rangle_{B_1}$ and $|2\rangle_B \rightarrow |1\rangle_{B_2}|0\rangle_{B_1}$. Base state $|0\rangle_{B_2}|0\rangle_{B_1}$ is not used.

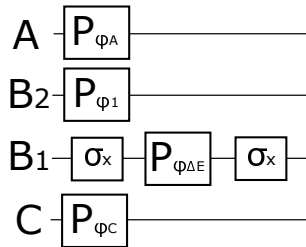


Figure 3. Scheme of the free evolution algorithm. Source: own work.

The free evolution of the system described by Eq. (1) is implemented by the algorithm showed in Fig. 3. Gates σ_x are standard NOT gates. Gates P_ϕ are standard phase-shift gates that operate according to the scheme:

$$|0\rangle \rightarrow |0\rangle, \quad |1\rangle \rightarrow e^{-i\phi}|1\rangle, \tag{10}$$

where: $\phi_A = E_A\hbar^{-1}dt$, $\phi_1 = E_1\hbar^{-1}dt$, $\phi_{\Delta E} = (E_2 - E_1)\hbar^{-1}dt$, $\phi_C = E_C\hbar^{-1}dt$ and dt is time step.

Implementation of the algorithm simulating interaction described by the Hamiltonian (3) is shown in the left drawing in Fig. 4. Three-input gates R_ϕ operate as follows:

$$|1\rangle|1\rangle|0\rangle \rightarrow \cos \phi |1\rangle|1\rangle|0\rangle + \sin \phi |1\rangle|1\rangle|1\rangle, \tag{11}$$

$$|1\rangle|1\rangle|1\rangle \rightarrow \cos \phi |1\rangle|1\rangle|1\rangle - \sin \phi |1\rangle|1\rangle|0\rangle, \tag{12}$$

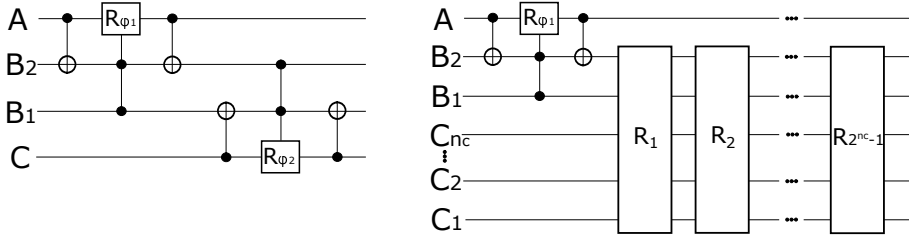


Figure 4. Scheme of the algorithm simulating interaction between subsystems. The left drawing shows the case for the Hamiltonian (3), while the right one shows the case for the Hamiltonian (7). Source: own work.

where $\phi_1 = |g_1|dt/\hbar$ and $\phi_2 = |g_2|dt/\hbar$.

Implementation of the interaction algorithm can be obtained by expressing the last two components from Eq. (9) in the following way:

$$\begin{aligned} \exp(-i(g_1\hat{a}^\dagger\hat{b}_1 + g_1^*\hat{a}\hat{b}_1^\dagger)dt/\hbar) &= \sum_{j=0}^{\infty} \frac{1}{j!} \left(-\frac{dt}{\hbar}\right)^j (g_1\hat{a}^\dagger\hat{b}_1 + g_1^*\hat{a}\hat{b}_1^\dagger)^j = \\ &= \sum_{j=0}^{\infty} \frac{(-1)^j}{(2j)!} \left(\frac{dt}{\hbar}\right)^{2j} (g_1\hat{a}^\dagger\hat{b}_1 + g_1^*\hat{a}\hat{b}_1^\dagger)^{2j} + \\ &\quad + i \sum_{j=0}^{\infty} \frac{(-1)^j}{(2j+1)!} \left(\frac{dt}{\hbar}\right)^{2j+1} (g_1\hat{a}^\dagger\hat{b}_1 + g_1^*\hat{a}\hat{b}_1^\dagger)^{2j+1} \end{aligned} \quad (13)$$

and using the following formulas:

$$(g_1\hat{a}^\dagger\hat{b}_1 + g_1^*\hat{a}\hat{b}_1^\dagger)^{2j}|0\rangle_A|1\rangle_B = |g_1|^{2j}|0\rangle_A|1\rangle_B, \quad (14)$$

$$(g_1\hat{a}^\dagger\hat{b}_1 + g_1^*\hat{a}\hat{b}_1^\dagger)^{2j}|1\rangle_A|0\rangle_B = |g_1|^{2j}|1\rangle_A|0\rangle_B, \quad (15)$$

$$(g_1\hat{a}^\dagger\hat{b}_1 + g_1^*\hat{a}\hat{b}_1^\dagger)^{2j+1}|0\rangle_A|1\rangle_B = |g_1|^{2j}g_1|1\rangle_A|0\rangle_B, \quad (16)$$

$$(g_1\hat{a}^\dagger\hat{b}_1 + g_1^*\hat{a}\hat{b}_1^\dagger)^{2j+1}|1\rangle_A|0\rangle_B = |g_1|^{2j}g_1^*|0\rangle_A|1\rangle_B. \quad (17)$$

The implementation of the algorithm simulating interaction of the extended system (described by the Hamiltonian (7)) is shown in the right drawing in Fig. 4. In this case, we simulate the subsystem C in n_c qubit subregister ($n_c = n_q - 3$). In each base state of the subregister, a single energy level is encoded. Therefore, the total number of energy levels of the subsystem C is equal to $n_L = 2^{n_c}$. The state $|0\rangle_C$ we identify with the vacuum state (lack of a photon). The transition $|1\rangle_B|0\rangle_C \leftrightarrow |0\rangle_B|i\rangle_C$ (the i -th component of the sum from the Hamiltonian (7)) is implemented by R_i block. The implementation of R_i blocks can be found in [9].

4. Simulation results

In the first part of our consideration, we examine our algorithm for the Hamiltonian (3) with conditions (4) and (5). As an initial state of the simulated system we choose $|1\rangle_A|0\rangle_B|0\rangle_C$. The simulation parameters are: $dt = 10^{-16}$ s, $E_A = E_1 = 2$ eV, $E_C = 0.2$ eV, and $E_2 = 1.8$ eV. The results are shown in Fig. 5. We only present the probabilities for the subsystem B, because $p_{A^*} = p_{B0}$ and $p_{C^*} = p_{B2}$.

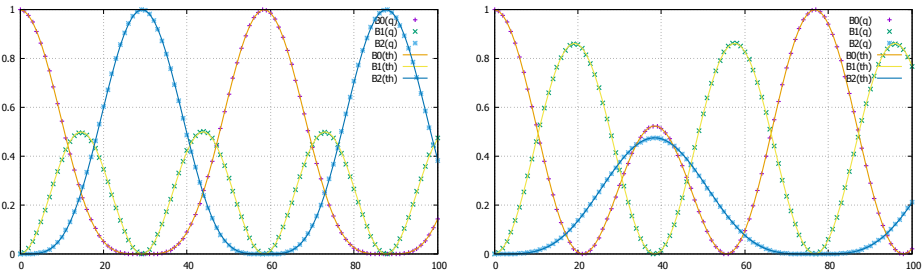


Figure 5. Probability of finding the system B in $|0\rangle_B$, $|1\rangle_B$ and $|2\rangle_B$ states as functions of time (in 10^{-15} s units). The left plot is made for $g_1 = g_2 = 0.05$ eV, the right one is made for $g_1 = 0.05$ eV and $g_2 = 0.02$ eV. The dotted lines shows the results of the simulation. Solids lines represent comparative theoretical results. Source: own work.

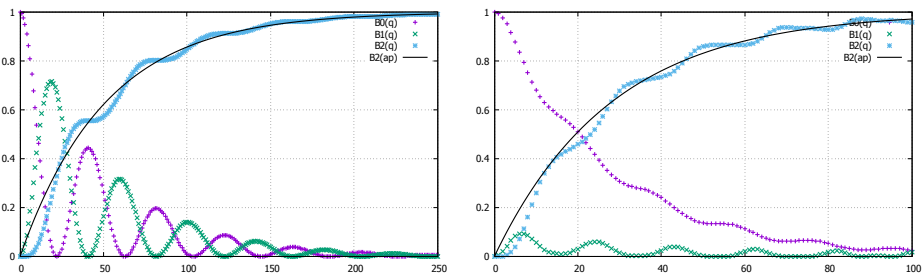


Figure 6. Probability of finding the system B in $|0\rangle_B$, $|1\rangle_B$ and $|2\rangle_B$ states as functions of time (in 10^{-15} s units). The left plot is made for $g_2 = 0.005$ eV, the right one is made for $g_2 = 0.02$ eV. The dotted lines shows the results of the simulation. Solids line represents result of exponential approximation. Source: own work.

In the next part of our consideration we examine the algorithm for the Hamiltonian (7) for $n_q = 9$ ($n_c = 6$). Other parameters take the following values: $dt = 10^{-16}$ s, $E_A = 2$ eV, $E_C = 0.2$ eV (center of the band), $E_1 = 2$ eV, $E_2 = 1.8$ eV

and $g_1 = 0.05\text{eV}$. The results of the simulation are shown in Fig. 6.

5. Conclusions

- In Fig. 5 we can see very good consistency of results obtained by the simulation and by the comparative method.
- In the case of the extended system C we can observe exponential growth of the state $|2\rangle_B$ occupation probability.

References

- [1] Feynman R., *Simulating physics with computers*, *Internat. J. Theor. Phys.*, 1982, vol. 21, pp. 467–488.
- [2] Shor P.W., *Algorithms for quantum computation: Discrete logarithm and factoring*, *Proc 35th Ann. Symp. Found. Comp. Sci., IEEE Comp.Soc. Pr.*, 1994, pp. 124–134.
- [3] Grover L.K., *From schrodinger equation to the quantum search algorithm*, *Am. J. Phys.*, 2001, vol. 69, pp. 769–777.
- [4] Schaetz T., Monroe C., Esslinger T., *Focus on quantum simulation*, *New Journal of Phys.*, 2013, vol. 15.
- [5] Kokail C., Maier C., van Bijnen R., *Self-verifying variational quantum simulation of lattice models*, *Nature*, 2019, vol. 569.
- [6] Jordan S., Lee K., Preskill J., *Quantum algorithms for quantum field theories*, *Science*, 2012, vol. 336, p. 1130–1133.
- [7] Dorfman K.E., Voronine D.V., *Photosynthetic reaction center as a quantum heat engine*, *PNAS*, 2013, vol. 110, no 8, p. 2746–2751.
- [8] G. S. Engel T.R.C., *Evidence for wavelike energy transfer through quantum coherence in photosynthetic systems*, *Nature*, 2007, vol. 446, no 12/04.
- [9] Ostrowski M., *Simulation of photon emission by an excited atom in the quantum register*, [In:] A. Wojciechowski, P. Napieralski, P. Lipiński (eds.), *TEWI 2021*, TUL Press, Lodz 2021, pp. 140–154.